JOURNAL OF CATALYSIS 74, 144–155 (1982)

Study on the Pulse Reaction Technique

VI. Kinetics of the Reaction of NO with NH_3 on a V_2O_5 Catalyst

AKIRA MIYAMOTO, YUTAKA YAMAZAKI, TADASHI HATTORI, MAKOTO INOMATA, AND YUICHI MURAKAMI

Department of Synthetic Chemistry, Faculty of Engineering, Nagoya University, Chikusa-ku, Nagoya 464, Japan

Received January 26, 1981; revised April 29, 1981

In order to examine the applicability of the rectangular pulse technique to the determination of the kinetics of a two-components' reaction on a catalyst in the specified surface state, the kinetics of the reaction of NO with NH_3 on the V_2O_5 catalyst, that is, $NO + NH_3 + V{=}O \rightarrow N_2 + H_2O + V{-}OH$, has been investigated using the rectangular pulse apparatus. Chromatograms of the individual components have shown that NH_3 is strongly adsorbed on the catalyst while NO or N_2 is not or only very weakly adsorbed. The adsorption of NH_3 has been approximately described by the Langmuir adsorption isotherm. The yield of N_2 produced by the reaction has changed significantly with the pulse width. This indicates a separation of NO and NH_3 in the catalyst bed during the pulse experiments. By analyzing the experimental data with the theory of the pulse technique, the kinetics of the above-mentioned two-components' reaction has successfully been determined and it has agreed with the kinetics of the reaction of NO with NH_3 under excess oxygen conditions determined by using the continuous flow technique. On the basis of these results, the rectangular pulse technique coupled with the theoretical analysis of the experimental data has been concluded to be a method effective for the determination of the kinetics of a multicomponents' reaction on a catalyst in the specified surface state.

INTRODUCTION

The pulse reaction technique has been widely used as a useful method in catalytic chemistry because this technique enables us to obtain experimental results rapidly and to observe the kinetic behaviors of a reaction on a catalyst in the specified surface state, such as a state in a given oxidation state or a state without the effect of products or residues (*1–3*). For many of the previous investigations using the pulse reaction technique, however, the kinetics of a reaction has not been determined quantitatively. This is because methods for the determination of the kinetics by using the pulse technique have not been well established for various types of reactions: As for the one component's reaction, the method has almost been established on the basis of the theory of the pulse technique and its comparison with the experimental data (*4–20*). As for the two-components' reaction, however, the method has not been established. This seems to be due to the following reason: When the pulse of a mixture of the two reactants is injected at the inlet of the catalyst bed, the separation of the reactants takes place in the catalyst bed because of the difference in the adsorption strength of the reactants. The separation of the two reactants in the catalyst bed then leads to a significant decrease in the rate of the reaction measured by using the pulse reaction technique. Furthermore, indefinite pulse width and indefinite concentrations of reactants in pulse for the conventional pulse experiments makes it more difficult to obtain quantitative, meaningful kinetic data from the pulse experiments. The theory of the pulse technique suggests that these problems can be overcome by using the rectangular pulse technique (*12, 13*), although this has not been verified experi-

0021-9517/82/030144-12$02.00/0

mentally. The purpose of this study is then to examine the applicability of the rectangular pulse technique to the determination of the kinetics of a two-components' reaction on a catalyst in the specified surface state, where the separation of reactants takes place in the catalyst bed during the pulse experiments. The effect of the separation of reactants or products has been experimentally investigated for the following type of reactions; $A_1 \rightleftharpoons A_2 + A_3$ (21–23). However, this has not been investigated for a two-components' reaction: Although some experimental studies have been done on the kinetics of the two-components' reactions, such as hydrogenations of ethylene and benzene (*10, 11, 24*), and oxidation of ethylene (*25*), the experimental results have been treated with the equation for one component's reaction and the separation of reactants in the catalyst bed has not been taken into consideration.

The reaction of NO and NH_3 (the NO–NH_3 reaction) on a V_2O_5 catalyst, that is, Reaction (1) below, was adopted as a test reaction, because Reaction (1) had been shown to be one of the stoichiometric reactions involved in the catalytic NO–NH_3 reaction on the vanadium oxide catalyst in the presence of O_2, which is composed of the following two stoichiometric reactions:

$$V{=}O + NH_3 + NO \rightarrow V{-}OH + N_2 + H_2O, \quad (1)$$

$$V{-}OH + \tfrac{1}{4}O_2 \rightarrow V{=}O + \tfrac{1}{2}H_2O, \quad (2)$$

where V=O is the vanadium–oxygen double bond on the surface (*26*). According to this mechanism, first the reaction of NO with NH_3 takes place at the V=O site on the surface to form N_2, H_2O, and V—OH [Reaction (1)]. The V—OH species on the surface is then reoxidized to the surface V=O by gaseous O_2 [Reaction (2)]. The kinetics of the catalytic NO–NH_3 reaction in the presence of O_2 has also been determined by using the continuous flow technique; the rate has been first order and zero order with respect to the concentrations of NO and NH_3, respectively. It has also been found using the infrared spectroscopy and TPD technique that NH_3 is strongly adsorbed on the surface, whereas NO is not or only very weakly adsorbed. In addition, a preliminary pulse experiment of the NO–NH_3 reaction on the V_2O_5 catalyst has indicated a very small yield of N_2 when the pulse width has been short (*27*). These data strongly suggest the separation of NO and NH_3 in the catalyst bed during pulse experiments. It should also be noted that the rate of the catalytic NO–NH_3 reaction under the excess oxygen condition is equal to the rate of Reaction (1). This means that the rate of Reaction (1) can also be determined by using the continuous flow technique; therefore, the validity of the kinetics of Reaction (1) determined using the rectangular pulse technique can be judged by its comparison with the kinetics of Reaction (1) determined using the continuous flow technique.

Reaction (1) is not a catalytic reaction but a stoichiometric reaction which forms the catalytic NO–NH_3 reaction in the presence of O_2. However, this does not decrease but increase the value of this study, because a heterogeneous catalytic reaction is usually composed of two or more steps; each step is a stoichiometric reaction involving one or more surface species on the catalyst as reactants. A detailed investigation of the individual stoichiometric reactions is necessary for understanding the mechanism of the catalytic reaction. In order to experimentally investigate the kinetics of such a stoichiometric reaction, the amount of gaseous reactant should be much smaller than that of the surface species on the catalyst, which is involved in the stoichiometric reaction as a reactant. This condition is hardly satisfied in experiments using the flow reaction technique, but can be easily attained in experiments using the pulse reaction technique. It should also be emphasized that, in the present study, experimental elaborations were made in order to produce the rectangular pulse of the mix-

ture of NO and NH_3 with a definite composition and a definite pulse width, and to observe the elution profile of N_2 formed by Reaction (1).

NOMENCLATURE

a	A factor which determines the shape of the inlet trapezium pulse (sec) (cf. Fig. 1)
b_A	Adsorption equilibrium constant of the Langmuir adsorption isotherm for A species (cm^3-bed/mol)
C_i	Concentration of component i(i = A, B, or R) in the gas phase (mol/cm^3-bed)
C_i^0	C_i at the inlet of the catalyst bed (mol/cm^3-bed)
k	Reaction rate constant (sec^{-1})
L	Catalyst bed length (cm)
q_A^0	Amount of adsorbed A species at full coverage (mol/cm^3-bed)
r	Reaction rate (mol/cm^3-bed sec)
t	Time (sec)
t_{Ar}	Time when the front of argon pulse arrives at the outlet TCD (sec) (cf. Fig. 3)
t_A, t_B	Time when the front of NH_3 or NO pulse arrives at the outlet TCD (sec) (cf. Figs. 4 and 5)
u	Moving velocity of carrier gas (cm-bed/sec)
Y_R	Yield of the product R (dimensionless)
W_p	Pulse width (sec)
z	Distance down catalyst bed (cm); at the inlet of the catalyst bed, $z = 0$; at the outlet, $z = L$
θ	Residence time of carrier gas defined by L/u (sec)
A	NH_3
B	NO
R	N_2

REACTION MODEL AND METHOD OF THEORETICAL ANALYSIS

Taking into account the results of the adsorption of NO and NH_3 described below and previous studies on the adsorptions of NO and NH_3 (*26*), a theoretical analysis was made on the basis of the following reaction model:

$$A(g) \overset{b_A}{\rightleftharpoons} A(ad), \tag{3}$$

$$A(ad) + B(g) \overset{k}{\rightarrow} R(g), \tag{4}$$

where A, B, and R stand for NH_3, NO, and N_2, respectively, while parenthetical g and ad refer to gaseous and adsorbed species, respectively. Furthermore, the following was assumed:

Assumption 1. The Langmuir adsorption equilibrium is established for A between the gas phase and the adsorbed phase, whereas neither reactant B nor product R is adsorbed on the catalyst.

Assumption 2. In the catalyst bed, the substance in the gas phase moves as a plug flow of linear velocity u together with the carrier gas.

Assumption 3. The influence of the mass transfer onto the catalyst surface is negligible.

Assumption 4. The amount of the produced N_2 (or R) is negligible compared to that of surface V=O bond.

Assumption 5. The effect of H_2O produced by Reaction (1) is negligible.

The validity of these assumptions will be proven later. According to the above-mentioned reaction model and assumptions, the basic equation expressing the mass balance of reactant A is given (*12, 13*) as follows:

$$\frac{\partial C_A}{\partial t} + \frac{q_A^0 b_A}{(1 + b_A C_A)^2} \frac{\partial C_A}{\partial t} = -u \frac{\partial C_A}{\partial z} - r. \tag{5}$$

The mass balance equations for B and R are different than the equation for A, since B or R is not adsorbed:

$$\frac{\partial C_B}{\partial t} = -u \frac{\partial C_B}{\partial t} - r, \tag{6}$$

$$\frac{\partial C_R}{\partial t} = -u \frac{\partial C_R}{\partial t} + r, \tag{7}$$

where r is the rate of the reaction and is

given by Eq. (8) in accordance with the reaction model.

$$r = \frac{kb_A C_A C_B q_A^0}{1 + b_A C_A}. \quad (8)$$

Since the mixture of the reactants A and B is fed as the rectangular pulse at the inlet of the catalyst bed, the boundary conditions at $z = 0$ are given as follows:

$$C_A = C_A^0, \quad C_B = C_B^0, \quad C_R = 0, \quad \text{when } 0 \le t \le W_p, \quad (9)$$

$$C_A = C_B = C_R = 0, \quad \text{when } t < 0 \text{ and } t > W_p, \quad (10)$$

where W_p is the width of the rectangular pulse. In order to take into account the deviation of the shape of the inlet pulse from rectangular, the boundary conditions shown in Fig. 1 are also used. Here, the shape of the inlet pulse is not rectangular, but trapezium. The value of a in Fig. 1 is determined from the shape of the pulse experimentally obtained.

The yield of R, Y_R, is defined as the ratio of the output amount of R to the input amount of B; therefore, Y_R is given by Eq. (11).

$$Y_R = \frac{\int_0^\infty C_R(t, L)\, dt}{\int_0^{W_p} C_B(t, 0)\, dt}, \quad (11)$$

where $C_R(t, L)$ is C_R at $t = t$ and $z = L$, while $C_B(t, 0)$ is C_B at $t = t$ and $z = 0$.

When A, B, or R is separately pulsed, the chromatogram of A, B, or R can be obtained, since neither component reacts on the catalyst in the absence of the reaction partner. The respective chromatograms of A, B, and R are described by Eqs. (12), (13), and (14), which are similar to Eqs. (5), (6), and (7):

$$\frac{\partial C_A}{\partial t} + \frac{q_A^0 b_A}{(1 + b_A C_A)^2} \frac{\partial C_A}{\partial t} = -u \frac{\partial C_A}{\partial z}, \quad (12)$$

$$\frac{\partial C_B}{\partial t} = -u \frac{\partial C_B}{\partial z}, \quad (13)$$

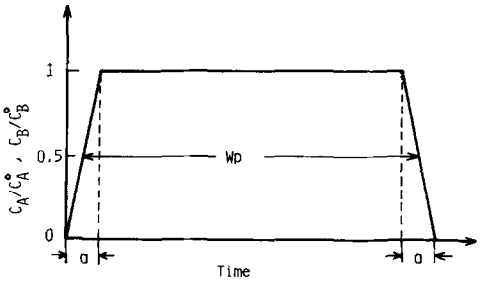

FIG. 1. Shape of the inlet pulse employed for the calculation. $a = 0$; rectangular inlet pulse. $a > 0$; trapezium inlet pulse.

$$\frac{\partial C_R}{\partial t} = -u \frac{\partial C_R}{\partial z}. \quad (14)$$

Calculations were made using the method of finite difference after transforming Eqs. (5)–(14) into dimensionless forms. The adsorption parameters, b_A and q_A^0, and the rate constant, k, were determined by using the least-squares method. Numerical calculations were carried out with a FACOM 230-75 computer (Computer Center, Nagoya University).

EXPERIMENTAL

Catalyst and Reagents

A V_2O_5 catalyst was prepared by the thermal decomposition of ammonium metavanadate at 500°C for 3 hr in a stream of O_2. The BET surface area of the catalyst was 5.4 m^2/g. A carrier gas (helium) was purified by the use of titanium metal sponge heated above 800°C, and a molecular sieve trap. Commercial NO (97.3% purity; impurities were 2.0% of N_2 and 0.7% of N_2O), NH_3 (99.9% purity), and O_2(99.8% purity) were used without further purification.

Apparatus and Procedure

The apparatus for the rectangular pulse technique employed in the present study is shown in Fig. 2. A sample gas of a given composition—which was confirmed by means of gas chromatography—was prepared and stored in two syringes (*4*), and filled the sampling loop of a six-way valve (*6*). The six-way valve was turned so that

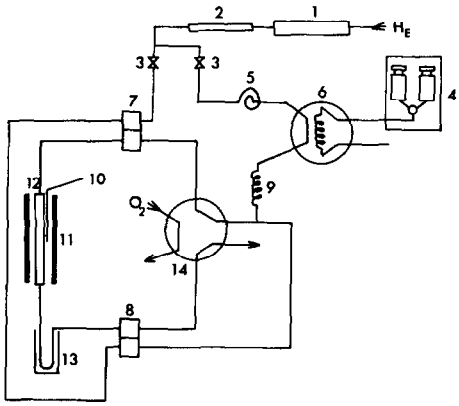

FIG. 2. Apparatus for the rectangular pulse technique. (1) Titanium metal sponge column; (2) molecular sieve trap; (3) pressure regulator; (4) 200-ml syringes for the preparation of a sample gas; (5) buffer tube; (6) six-way valve for sampling; (7) TCD at the inlet of reactor; (8) TCD at the outlet of reactor; (9) capillary; (10) thermocouple; (11) electric furnace; (12) reactor; (13) liquid nitrogen trap; (14) six-way valve for the treatment with O_2.

the sample gas in the sampling loop could be pushed out through a stainless-steel capillary (*9*) to the main stream of the carrier gas, to then be carried to the reactor (*12*). Before all of the sample gas in the sampling loop was pushed out from the sampling loop, the six-way valve (*6*) was returned. In such a way, the rectangular pulse could be obtained; the concentration was varied by changing the composition of the sample gas, the flow rates of the carrier gas, and the pusher gas. The pulse width was varied by changing the time interval between turning and returning the six-way valve. The shape of the input pulse was recorded by a thermal conductivity detector (*7*). The $NO-NH_3$ reaction under the present experimental condition produced N_2 and H_2O selectively, according to Reaction (1). The effluents were carried to a liquid nitrogen trap (*13*). It was confirmed that NO, NH_3, N_2O, and H_2O were substantially trapped, while the shape of N_2 pulse was not deformed by this trap. Thus, it was possible to observe the elution profile of N_2 at the outlet of the catalyst bed by a thermal conductivity detector (*8*). According to Eq. (11), the yield of N_2, Y_R, was calculated from the elution profile of N_2 as the ratio of the amount of produced N_2 to that of NO supplied. When only NO or NH_3 was pulsed in order to observe the chromatogram of NO or NH_3, the trap (*13*) was not employed. Between the pulses of reactants (mixtures of NO and NH_3) or adsorbates (NO or NH_3), the catalyst was treated with O_2 gas stream at 500°C in order to hold the oxidation state of the catalyst in the highest oxidation state, i.e., V_2O_5, and in order to remove any adsorbates on the catalyst.

Unless otherwise specified, experiments of the $NO-NH_3$ reaction and adsorptions of NO, NH_3, N_2, and Ar were carried out under the following conditions: Catalyst weight = 4.0 g. Dimension of catalyst particles = 28–48 mesh. Reaction temperature = 150°C. Flow rate of the carrier gas = 150 cm^3/min. Inlet concentration of NO (C_B^0) = 2.39×10^{-8} mol/cm^3-bed. Initial concentration of NH_3 (C_A^0) = $2.39–47.7 \times 10^{-8}$ mol/cm^3-bed. Pulse width (W_p) = 10–60 sec. Void fraction of the catalyst bed = 0.706. Residence time in the catalyst bed (θ) = 1.14 sec.

EXPERIMENTAL RESULTS

Production of Rectangular Pulse

It was confirmed that a rectangular pulse could be obtained with the described apparatus by using argon as a sample gas. As shown in Fig. 3a, the chromatogram of an argon pulse at the inlet was rectangular, which indicates that the apparatus worked well. The shape of the inlet pulse was rectangular for all of NO, NH_3, and N_2, irrespective of the pulse width or the inlet concentration employed (Figs. 4a, 5a, and 5c). The chromatogram of argon pulse at the outlet shown in Fig. 3b was almost the same as that at the inlet shown in Fig. 3a, except for the time lag, which was equal to the residence time between the two detectors shown as (7) and (8) in Fig. 2. A closer inspection of the chromatograms in Figs. 3a and b shows that the outlet chromatogram

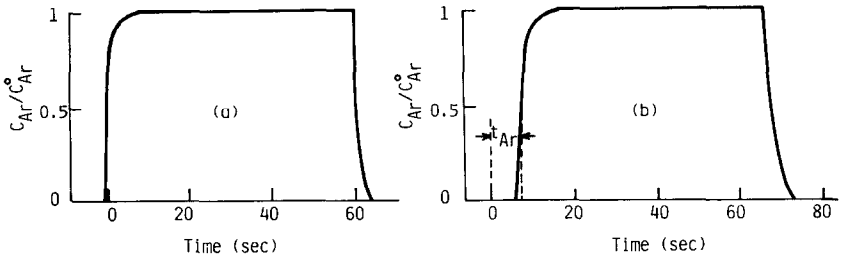

FIG. 3. Chromatograms of argon pulses at the inlet (a) and the outlet (b) of the reactor. C_{Ar}: Concentration of argon. $C_{Ar}{}^{0}$: Inlet concentration of argon at the plateau of the rectangular pulse. $C_{Ar}{}^{0} = 9.54 \times 10^{-8}$ mol/cm³-bed. $W_p = 60$ sec. Temperature = 150°C. Catalyst weight = 4.0 g.

of argon pulse is slightly broader than the inlet one at the front and the tail of the pulse, indicating the dispersion of argon pulse taking place in the space between the two detectors. By measuring the chromatograms of argon under various experimental conditions, with or without the V_2O_5 catalyst, it was found that the broadening of the argon pulse mainly takes place in the space except for the catalyst bed, and the dispersion of argon pulse in the catalyst bed is negligible. This is reasonable since the residence time between the two detectors was about 7 sec while that in the catalyst bed (θ) was calculated to be 1.14 sec.

Adsorptions of NO, NH_3, and N_2

No decomposition of NO or NH_3 was observed. Figure 4b shows the shape of the outlet NO pulse. As shown, this was equal to the shape of the outlet argon pulse shown in Fig. 3b: The close inspection by overlaying did not indicate any noticeable difference between the shape of the outlet NO pulse and that of the outlet argon pulse. Furthermore, the residence time of the NO pulse between the two detectors (t_B in Fig. 4b) was equal to that of the argon pulse (t_{Ar} in Fig. 3b) within experimental errors. Similar data were obtained for NO pulses with various pulse widths and with various concentrations in pulse. These results indicate that NO is not or only very weakly adsorbed on the catalyst. Similarly, the chromatograms of N_2 showed that N_2 is not or only very weakly adsorbed on the V_2O_5 catalyst.

The shape of NH_3 pulses at the outlet of the catalyst bed was markedly different from that at the inlet, suggesting that NH_3 is strongly adsorbed on the catalyst. Solid lines in Fig. 5 show two examples of the outlet chromatograms of NH_3 measured at various concentrations of NH_3 in pulse. As shown in Fig. 5, the time lag between the inlet and the outlet pulses (t_A) was significantly longer than that for the argon pulse (t_{Ar}), and the shape of the outlet NH_3 pulse was deformed markedly from the rec-

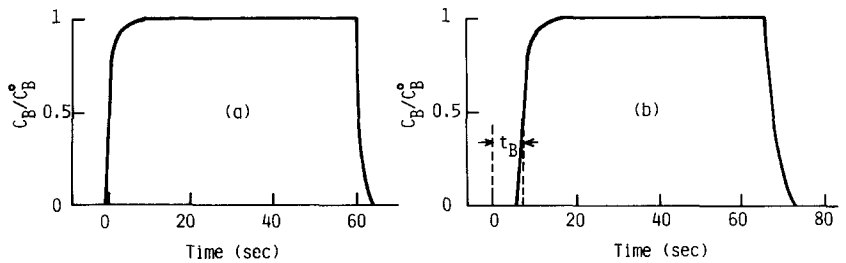

FIG. 4. Chromatograms of NO pulses at the inlet (a) and the outlet (b) of the reactor. $C_B{}^{0} = 9.54 \times 10^{-8}$ mol/cm³-bed. $W_p = 60$ sec. Temperature = 150°C. Catalyst wieght = 4.0 g.

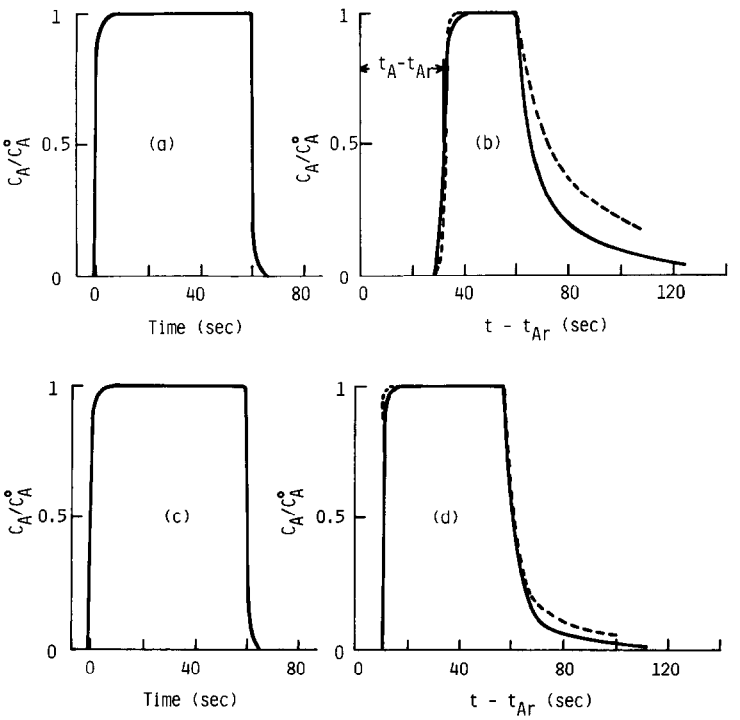

FIG. 5. Chromatograms of NH_3 at the inlet (a and c) and the outlet (b and d) of the reactor. Solid line, experimental. Broken line, calculated. W_p = 60 sec. Temperature = 150°C. Catalyst weight = 4.0 g. (a) and (b), $C_A^0 = 1.43 \times 10^{-7}$ mol/cm³-bed. (c) and (d), $C_A^0 = 4.77 \times 10^{-7}$ mol/cm³-bed.

tangular pulse introduced. Furthermore, the t_A was dependent on the inlet concentration of NH_3 in pulse; as the inlet concentration of NH_3 decreased the t_A increased.

The NO–NH_3 Reaction on the V_2O_5 Catalyst

Results of the NO–NH_3 reaction on the V_2O_5 at various inlet concentrations of NH_3, C_A^0, and various pulse widths, W_p, are shown in Figs. 6 and 7. The inlet concentration of NO, C_B^0, was constant for all of the experiments shown in Figs. 6 and 7; $C_B^0 = 2.39 \times 10^{-8}$ mol/cm³-bed. The closed circles in Fig. 6 indicate the experimental relationship between the yield of N_2, Y_R, and W_p at various C_A^0. The solid lines in Fig. 7 indicate the elution profiles of N_2 experimentally observed at various C_A^0. When C_A^0 was as low as 2.39×10^{-8} mol/cm³-bed, as shown in Fig. 6a, Y_R was very small at W_p = 10 or 20 sec and in-

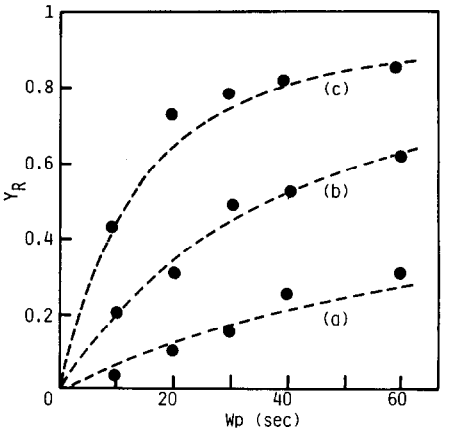

FIG. 6. Effect of pulse width (W_p) on the yield of N_2 (Y_R). Closed circle, experimental. Broken line, calculated. (a) $C_A^0 = 2.39 \times 10^{-8}$ mol/cm³-bed. $C_B^0 = 2.39 \times 10^{-8}$ mol/cm³-bed. (b) $C_A^0 = 4.77 \times 10^{-8}$ mol/cm³-bed. $C_B^0 = 2.39 \times 10^{-8}$ mol/cm³-bed. (c) $C_A^0 = 1.43 \times 10^{-7}$ mol/cm³-bed. $C_B^0 = 2.39 \times 10^{-8}$ mol/cm³-bed. Temperature = 150°C. Catalyst weight = 4.0 g.

creased linearly with increasing W_p. In Fig. 7a, the elution profile of N_2, that is, C_R/C_B^0, is shown for the pulse with $C_A^0 = 2.39 \times 10^{-8}$ mol/cm³-bed and $W_p = 60$ sec. C_R/C_B^0 increased monotonically with t in the region $0 \leq (t - t_{Ar}) \leq 60$ sec, and decreased abruptly at $(t - t_{Ar}) \approx 60$ sec. When the pulse width was small, the elution profile of N_2 was almost the same as that at $W_p = 60$ sec, except that the break-down point was small in accordance with the pulse width. The dotted line in Fig. 7a shows an example of such profiles. Figures 6b and 7b show the results of the NO–NH_3 reaction at $C_A^0 = 4.77 \times 10^{-8}$ mol/cm³-bed, which is twice as high as the concentration shown in Figs. 6a and 7a. Compared with the data shown in Figs. 6a and 7a, it should be noted that both Y_R and C_R/C_B^0 for $C_A^0 = 4.77 \times 10^{-8}$ mol/cm³-bed are higher than those for $C_A^0 = 2.39 \times 10^{-8}$ mol/cm³-bed. When C_A^0 increased further, i.e., $C_A^0 = 1.43 \times 10^{-7}$ mol/cm³-bed, which is six times as high as the concentration shown in Figs. 6a and 7a,

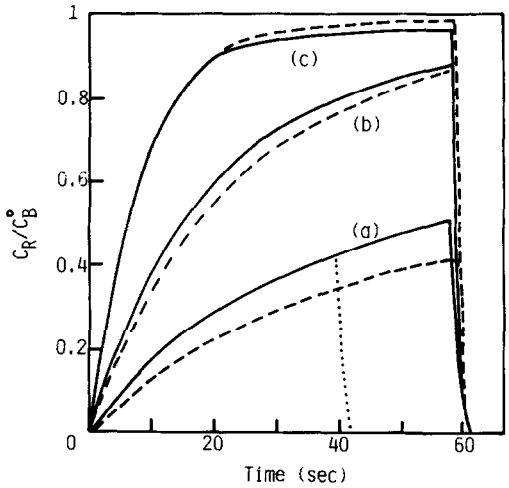

FIG. 7. Elution profiles of N_2. Solid line, experimental profile at $W_p = 60$ sec. Dotted line, experimental profile at $W_p = 40$ sec. Broken line, calculated profile at $W_p = 60$ sec. (a) $C_A^0 = 2.39 \times 10^{-8}$ mol/cm³-bed. $C_B^0 = 2.39 \times 10^{-8}$ mol/cm³-bed. (b) $C_A^0 = 4.77 \times 10^{-8}$ mol/cm³-bed. $C_B^0 = 2.39 \times 10^{-8}$ mol/cm³-bed. (c) $C_A^0 = 1.43 \times 10^{-7}$ mol/cm³-bed. $C_B^0 = 2.39 \times 10^{-8}$ mol/cm³-bed. Temperature = 150°C. Catalyst weight = 4.0 g.

Y_R rose rapidly at $0 \leq W_p \leq 20$ sec and exhibited no further increase at $W_p > 20$ sec, as indicated in Fig. 6c. Similar phenomena can also be observed in the elution profile of N_2 shown in Fig. 7c. That is, C_R/C_B^0 grew abruptly at $0 \leq (t - t_{Ar}) \leq 20$ sec and showed no further increase at $20 < (t - t_{Ar}) \leq 60$ sec.

DISCUSSION

Validity of the Assumptions Made in the Calculations

As mentioned above, several assumptions were made in the theoretical calculations. All of these assumptions are valid under the present experimental conditions:

Assumption 1. The validity of this assumption will be proven below by the comparison of the experimental chromatogram of NH_3, NO, or N_2 with the theoretical one (cf. Figs. 4 and 5).

Assumption 2. As mentioned above, the dispersion of the argon pulse in the catalyst bed is negligible. Therefore, the deviation from the plug flow condition is minimal in the catalyst bed. Although a slight dispersion of the argon pulse takes place in the vacant space except for the catalyst bed, this is taken into consideration in the calculations as the shape of the inlet pulse (cf. Fig. 1).

Assumption 3. Experiments using catalyst particles of different dimensions, i.e., 16–28 mesh and 48–65 mesh, gave the same results as those shown above, in which the particles of 28–48 mesh were used.

Assumption 4. The concentrations of reactants were so low that the catalyst bed can be regarded isothermal.

Assumption 5. The amount of N_2 produced was at most 12% of the amount of the surface V=O on the catalyst.

Assumption 6. By using the temperature-programmed desorption technique, the adsorption of H_2O was confirmed to be significantly weaker than that of NH_3. Furthermore, the amount of the produced H_2O

was calculated to be at most 30% of that of NH_3 fed and 12% of the amount of the surface V=O on the catalyst.

Determination of Adsorption Parameters

Eberly *et al.* (*28, 29*) have investigated the adsorption of hydrocarbons or NH_3 on various catalysts using a technique similar to that employed in this study. According to their method of analysis, the chromatograms of NH_3 shown in Fig. 5 indicate that NH_3 is strongly adsorbed on the V_2O_5 catalyst. When the adsorption is infinitely strong, that is, when the adsorption equilibrium constant is infinite, the amount of the adsorbed NH_3 at full coverage, q_A^0, can be calculated by the following equation (*14*):

$$q_A^0 = C_A^0 (t_A - t_{Ar})/\theta. \quad (15)$$

If the adsorption of NH_3 on the catalyst is infinitely strong, the value of q_A^0 should be constant irrespective of C_A^0. Figure 8 shows the experimental relationship between q_A^0 and the reciprocal of C_A^0. Here, q_A^0 was calculated from the measured t_A on the basis of Eq. (15). As shown, q_A^0 thus calculated was not constant but decreased linearly with an increase in $1/C_A^0$. Therefore, the adsorption of NH_3 on the catalyst is not infinitely strong. The Langmuir adsorption isotherm with finite adsorption coefficient can then be applied to the system. Numerical calculations were made for various b_A, q_A^0, and C_A^0 in order to obtain theoretical chromatograms of NH_3 by the least-squares method. The calculated chromatograms were then compared with the experimental ones shown for example in Fig. 5, and the following adsorption parameters of the Langmuir adsorption isotherm were determined:

$$b_A = 4.12 \times 10^7 \text{ cm}^3\text{-bed/mol}, \quad (16)$$

$$q_A^0 = 4.85 \times 10^{-6} \text{ mol/cm}^3\text{-bed}. \quad (17)$$

The broken lines in Fig. 5 are the chromatograms of NH_3 calculated on the basis of Eq. (12) together with these parameters. As shown, the calculated chromatograms of NH_3 almost agree with the experimental ones shown by the solid lines except for the tailing part where the calculated value is larger than the observed one. It should be noted that the calculated chromatogram of NH_3 does not change significantly even if the trapezium pulse (a = 3 sec; Fig. 1) instead of the rectangular pulse is used as the inlet pulse. The discrepancy at the tailing part cannot lead to a significant error in determining the kinetics of Reaction (1). This is because Reaction (1) does not take place at $(t - t_{Ar}) > W_p$ (cf. for example Fig. 7), while the tailing of the outlet NH_3 pulse takes place at $(t - t_{Ar}) > W_p$. On the basis of this reason, the tailing part was not taken into consideration in the least-squares calculations to determine the adsorption parameters. It should also be noted that the adsorption parameters are consistent with the data shown in Fig. 8: According to the equation of the Langmuir adsorption isotherm, infinitely high concentration leads to the same results as the results for infinitely strong adsorption. In other words, the intercept of the plot shown in Fig. 8 should be equal to q_A^0 determined by the Langmuir adsorption isotherm. This is in accordance with the experimental results, since the intercept in Fig. 5, that is, 4.4×10^{-6}

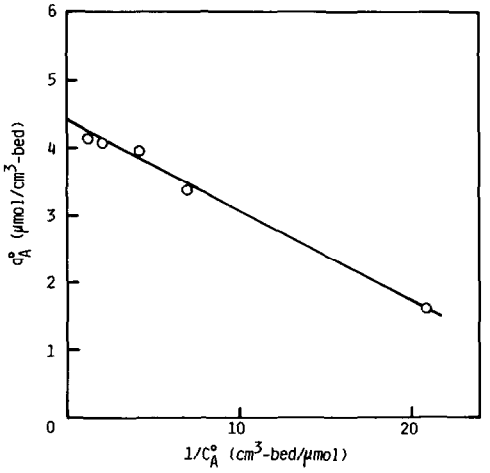

FIG. 8. Relationship between q_A^0 calculated by Eq. (15) and $1/C_A^0$.

mol/cm³-bed, was close to the value of q_A^0 shown in Eq. (17). Thus, we can note that the adsorption of NH_3 on the V_2O_5 catalyst is approximately described by the Langmuir adsorption isotherm.

The shape of the outlet NO pulse was equal to that of the outlet argon pulse as shown in Figs. 3b and 4b. Furthermore, the calculations of chromatograms for NO indicate that the adsorption equilibrium constant for NO is at least 10^2–10^3 times smaller than that for NH_3. This means that NO is not or only very weakly adsorbed on the catalyst. It was similarly proven that N_2 is not or only very weakly adsorbed on the catalyst. These data are in accordance with the reaction model shown by Eqs. 3 and 4.

Determination of the Rate Constant and Soundness of the Parameters Determined

As shown in Fig. 6, the Y_R is not constant but increases monotonically with W_p. Similarly, the shape of the outlet N_2 pulse (or the C_R/C_B^0) in Fig. 7 deviates significantly from that of the inlet rectangular pulse. These data coupled with the behaviors of NO and NH_3 in adsorption suggest that a considerable separation of NO and NH_3 takes place in the catalyst bed. This means that the steady-state kinetics cannot be applied to this system. Therefore, the theory of the pulse reaction technique, i.e., Eqs. (5)–(11), is applied to the determination of the kinetics of Reaction (1). The adsorption parameters, b_A and q_A^0, have already been determined. The rate constant, k, is then determined on the basis of the experimental data of Y_R by the least-squares method as follows:

$$k = 1.33 \times 10^6 \text{ cm}^3\text{-bed/mol sec.} \quad (18)$$

The broken lines shown in Fig. 6 are relationships between Y_R and W_p calculated on the basis of the parameters, b_A, q_A^0, and k, determined. Under all experimental conditions shown in Fig. 6, the calculated Y_R agrees with the experimental one. Furthermore, the calculated elution profile of N_2, that is, C_R/C_B^0, agrees with the experimental profile; some examples of the comparison between the calculated and the experimental profiles are shown in Fig. 7. It should be noted that relationships between Y_R and W_p and elution profiles of R obtained for the rectangular inlet pulse were calculated to be almost the same as those obtained for the trapezium inlet pulse (a = 3 sec; Fig. 1). These data indicate the soundness of parameters determined.

In this study, the adsorption parameters, b_A and q_A^0, were determined from the chromatograms of NH_3. It is also possible to determine all of the parameters, b_A, q_A^0, and k, only from the measured relationships between Y_R and W_p by the least-squares method, when the data of the chromatograms of individual reactants are not available. The agreement between the theory and experiments shown in Figs. 6 and 7 assures the applicability of the latter method.

Comparison of the Kinetics of Reaction (1) Determined Using the Pulse Reaction Technique with That Determined Using the Flow Reaction Technique

The catalytic NO–NH_3 reaction on vanadium oxide catalyst in the presence of O_2 has been shown to be composed of two stoichiometric reactions, i.e., Reactions (1) and (2). Under the excess oxygen condition, Reaction (2) proceeds rapidly and Reaction (1) becomes the rate-determining step (*26*). Therefore, the kinetics of Reaction (1) can be determined separately by measuring the rates of the NO–NH_3 reaction using the flow reaction technique, and it can be compared with the kinetics of Reaction (1) determined by using the rectangular pulse technique. According to the kinetic data obtained by using the flow reaction technique (*26*), the rate of the reaction under the excess oxygen condition was of the first order and zero order with respect to the concentrations of NO and NH_3, respectively, which suggests that Re-

action (1) is a reaction between a strongly adsorbed NH_3 and a gaseous NO. This is in accordance with the above-mentioned kinetics of Reaction (1) determined by using the pulse reaction technique. In addition, the present study using the pulse reaction technique indicates that the adsorption of NH_3 on the catalyst is not irreversible, but reversible; the Langmuir adsorption isotherm can approximately be applied to the adsorption. This agrees with the results of the adsorption of NH_3 obtained by using the temperature programmed desorption technique; a desorption peak of NH_3 with its maximum at 180°C has been observed (*26*). The rate equation shown by Eq. (8) indicates the first order kinetics with respect to the concentration of NO, C_B. The data of Y_R obtained using the rectangular pulse technique at various $C_B°$ agreed with the rate equation, although $C_B°$ could not be varied extensively. This is because Assumption 4 was not satisfied when $C_B°$ was high. The rate constant of the NO–NH_3 reaction under the excess oxygen condition has been determined using the flow reaction technique at temperatures between 180 and 330°C (*26*). The extrapolation of the Arrhenius equation for the rate constant, together with the corrections due to the Langmuir adsorption isotherm for NH_3, leads to the rate constant at 150°C:

$$k = 8.0 \times 10^5 \text{ cm}^3\text{-bed/mol} \cdot \text{sec.} \quad (19)$$

This value is approximately equal to the rate constant determined by using the pulse reaction technique shown by Eq. (18), since the difference between the rate constants shown by Eqs. (18) and (19) corresponds to the difference in the activation energy by only 0.4 kcal/mol. Consequently, the kinetics of Reaction (1) determined using the flow reaction technique agrees with that determined using the pulse reaction technique. This supports the validity of the present study and indicates the applicability of the rectangular pulse technique to the investigation of the kinetics of a two-components' reaction on a catalyst in the specified surface state.

CONCLUSIONS

The kinetics of a stoichiometric reaction [Reaction (1)] involved in the catalytic NO–NH_3 reaction in the presence of O_2—a two-components' reaction on a catalyst in the specified oxidation state—has been determined by using the rectangular pulse apparatus, and the kinetics thus determined has agreed with that determined by using the continuous flow technique. The results of the rectangular pulse experiments have shown the presence of the separation of NO and NH_3 in the catalyst bed; however, this problem has successfully been overcome by analyzing the experimental data with the theory of the pulse technique. This indicates the applicability of the rectangular pulse technique to the investigation of the kinetics of a two-components' reaction on a catalyst in the specified surface state, where the separation of reactants takes place in the catalyst bed. Although only a two-components' reaction between a strongly adsorbed species and a gaseous species has been treated in this study, the present study assures further applications of the rectangular pulse technique to the investigation of the kinetics of various types of multicomponents' reactions on catalysts in specified surface states, such as a state in a given oxidation state or a state without the effects of residues or products. This paper provides an example of what should be done for the investigation of these kinetics by the pulse technique.

REFERENCES

1. Murakami, Y., *in* "Some Theoretical Problems of Catalysis" (T. Kwan, G. K. Boreskov, and K. Tamaru, Eds.), p. 203. University of Tokyo Press, Tokyo, 1973.
2. Galeski, J. B., and Hightower, J. W., *Canad. J. Chem. Eng.* **48**, 151 (1970).
3. Furusawa, T., Suzuki, M., and Smith, J. M., *Catal. Rev.* **13**, 43 (1976).
4. Bassett, D. W., and Habgood, H. W., *J. Phys. Chem.* **64**, 769 (1960).

5. Roginskii, S. Z., Yanovskii, M. I., and Gasiev, G. A., *Kinet. Katal.* **3,** 529 (1962).
6. Gasiev, G. A., Falinovskii, V. Yu., and Yanovskii, M. I., *Kinet. Katal.* **4,** 688 (1963).
7. Schwab, G. M., and Watson, A. M., *J. Catal.* **4,** 570 (1965).
8. Echigoya, E., and Ochiai, Y., *Kogyo Kagaku Zassi* **69,** 1858 (1966).
9. Bett, J. A. S., and Hall, W. K., *J. Catal.* **10,** 105 (1968).
10. Blanton, W. A., Jr., Byers, C. H., and Merrill, R. P., *Ind. Eng. Chem. Fund.* **7,** 611 (1968).
11. Toyota, K., and Echigoya, E., *Kagaku Kogaku* **32,** 1005 (1968).
12. Hattori, T., and Murakami, Y., *J. Catal.* **10,** 114 (1968).
13. Hattori, T., and Murakami, Y., *J. Catal.* **12,** 166 (1968).
14. Hattori, T., and Murakami, Y., *J. Catal.* **31,** 127 (1973).
15. Hattori, T., and Murakami, Y., *J. Catal.* **33,** 365 (1974).
16. Makar, K., and Merrill, R. P., *J. Catal.* **24,** 546 (1972).
17. Hattori, T., and Murakami, Y., *Canad. J. Chem. Eng.* **52,** 601 (1974).
18. Hattori, T., Kanetake, K., and Murakami, Y., *Nippon Kagaku Kaishi* **1977,** 1597 (1977).
19. Murakami, Y., Niwa, M., Hattori, T., Osawa, S., Igushi, I., and Ando, H., *J. Catal.* **49,** 83 (1977).
20. Mori, T., Masuda, H., Imai, H., and Murakami, Y., *Nippon Kagaku Kaishi* **1979,** 1449 (1979).
21. Matsen, J. M., Harding, J. W., and Magee, E. M., *J. Phys. Chem.* **69,** 522 (1965).
22. Murakami, Y., Hattori, T., and Hattori, T., *J. Catal.* **10,** 123 (1968).
23. Schweich, D., and Villermaux, J., *Ind. Eng. Chem. Fund.* **17,** 1 (1978).
24. Sica, A. M., Valles, E. M., and Gigola, C. E., *J. Catal.* **51,** 115 (1978).
25. Verma, A., and Kalinguine, S., *J. Catal.* **30,** 430 (1973).
26. Inomata, M., Miyamoto, A., and Murakami, Y., *J. Catal.* **62,** 140 (1980).
27. Miyamoto, A., Yamazaki, Y., and Murakami, Y., *Nippon Kagaku Kaishi* **1977,** 619 (1977).
28. Eberly, P. E., Jr., and Kimberlin, C. N., Jr., *Trans. Faraday Soc.* **57,** 1169 (1961).
29. Eberly, P. E., Jr., *J. Phys. Chem.* **65,** 1261 (1961).